

## Why does pulmonary venous pressure rise after onset of LV dysfunction: a theoretical analysis

DANIEL BURKHOFF AND JOHN V. TYBERG

*Division of Circulatory Physiology, Department of Medicine, Columbia Presbyterian Hospital, New York, New York 10032; and Departments of Internal Medicine and Medical Physiology, University of Calgary Health Sciences Centre, Calgary, Alberta T2N 4N1, Canada*

**Burkhoff, Daniel, and John V. Tyberg.** Why does pulmonary venous pressure rise after onset of LV dysfunction: a theoretical analysis. *Am. J. Physiol.* 265 (*Heart Circ. Physiol.* 34): H1819-H1828, 1993.—One of the most important consequences of acute left ventricular dysfunction (LVD) is pulmonary edema resulting from a rise in pulmonary venous pressure (PVP). It is generally believed that the PVP rise is a direct hemodynamic consequence of LVD. While this paradigm seems plausible, especially if the LV is viewed as a sump pump, there is no specific evidence to support this simple explanation. A theoretical analysis was performed to assess the hemodynamic mechanisms responsible for the dramatic rise in PVP after acute LVD. The ventricles were modeled as time-varying elastances; pulmonary and systemic vascular systems were modeled as series of resistive and capacitive elements. In response to a 50% decrease in LV contractile strength [end-systolic elastance ( $E_{es}$ )], cardiac output (CO) and mean arterial pressure (MAP) dropped substantially, while PVP increased minimally from its baseline of 12 to  $\sim$ 15 mmHg. With LV  $E_{es}$  set at 50% of normal, the effects of sympathetic activation were tested. When heart rate and total peripheral resistance were increased, CO and MAP improved, yet PVP still did not rise. The only intervention that caused a substantial increase in PVP was to simulate the decrease in unstressed volume ( $V_U$ ) of the venous system known to occur with sympathetic activation. When  $V_U$  was decreased by about 15–20% (comparable to experimentally observed shifts with acute heart failure), PVP increased above 25 mmHg. The effects of pericardial constraints were investigated, and the results suggest a major role of this organ in determining the overall hemodynamic response to acute LVD, sympathetic activation, and explaining the responses to therapy. Thus this analysis suggests that elevations of PVP do not occur simply as a direct hemodynamic consequence of acute LVD. Rather, changes in PVP may be dictated more by sympathetic control on venous capacity. If confirmed, recognition of this as a primary mechanism may prove important in directing development of new therapies and in understanding the mechanisms of disease progression in heart failure.

venous system; sympathetic nervous system; pericardium; cardiovascular model

ONE OF THE MOST common and devastating consequences of acute left ventricular dysfunction (LVD) is pulmonary edema. Increased pulmonary venous pressure accompanying ventricular failure causes transudation of fluid into the pulmonary capillary interstitium, which limits the transfer of oxygen from alveoli into blood. The resulting hypoxia (and sometimes acidosis) can lead to further deterioration of ventricular performance and to further decreases in body tissue oxygenation.

Despite the longstanding recognition of the correlation between acute LVD and the development of pulmonary congestion, significant gaps exist in our understanding of the mechanisms by which pulmonary capillary pressure increases when the pumping ability of the ventricle is suddenly impaired. It is generally believed that fluid buildup in the lungs results from shifting blood from the peripheral circulation to the central (i.e., heart-lung) compartment (9, 13, 22); this shift of volume is generally believed to be a direct hemodynamic consequence of the decreased pumping ability of the ventricle (9, 34, 40). This hypothesis assigns only a minor role to the many changes that occur in the cardiovascular system when heart function deteriorates acutely. Decreases in blood pressure and cardiac output cause rapid activation of neurohormonal systems which, among other things, causes acute increases in heart rate, increased arterial resistance, and a decrease in capacity of the venous system (2–6, 8, 27, 34). However, it is unknown whether and to what extent these reflex-mediated changes in the cardiovascular system properties play a significant role in elevating pulmonary venous pressure. This gap in understanding may exist because independent control of each of the factors involved is not possible in the intact organism (human or experimental animal), making it difficult to separate the relative contributions of the different components of the system.

The purpose of this theoretical analysis, therefore, was to assess the relative importance of decreased ventricular contractile state, increased heart rate, increased arterial resistance, and decreased venous capacity in the development of pulmonary congestion after the onset of acute LVD. This was accomplished using a computer-based analysis of cardiovascular hemodynamics in which each parameter of interest can be varied independently or in combination with others. The results of this analysis suggest that the most important factor causing an increase in pulmonary capillary pressure is the decrease in venous capacity, which in turn leads to a marked increase in the effective circulating blood volume. Importantly, it is shown that in the absence of such changes in venous capacity, pulmonary capillary pressure rises very little as a direct hemodynamic consequence of acute LVD even in combination with increases in arterial resistance and heart rate. Finally, the

results of the analysis emphasize a major role of the pericardium in restricting ventricular filling when venous pressure rises, and in explaining the clinically observed hemodynamic responses to venodilators. The limitations of the analysis are discussed.

## METHODS

**Theoretical considerations.** The cardiovascular system was modeled as shown in Fig. 1. The details of this model are provided in APPENDIX A and elsewhere (29); only a brief description is provided here. The right and left ventricular pumping characteristics are represented by modifications of the time-varying elastance [ $E(t)$ ] theory of chamber contraction, which relates instantaneous ventricular pressure [ $P(t)$ ] linearly to instantaneous volume [ $V(t)$ ]:  $P(t) = E(t)[V(t) - V_0]$ , where  $V_0$  is the volume at which end-systolic pressure ( $P_{es}$ ) is equal to 0 mmHg. The  $E(t)$  function is modeled as a raised sine wave during systole and an exponential decay during diastole (with time constant of relaxation  $\tau$ ). This representation of LV function was modified to account for the fact that there is a nonlinear relationship between end-diastolic ventricular pressure ( $P_{ed}$ ) and volume ( $V_{ed}$ ) that was assumed to be an exponential function:  $P_{ed} = A \exp\{[B(V_{ed} - V_0)] - 1\}$  (29). With this ventricular model, contractility is indexed by end-systolic elastance ( $E_{es}$ ), which is the maximal value of the  $E(t)$  function (13); the time at which  $E_{es}$  is reached is defined as the time of end systole ( $T_{es}$ ).

The systemic and pulmonary circuits are each modeled by lumped venous ( $C_v$ ) and arterial capacitances ( $C_a$ ); a proximal characteristic resistance ( $R_c$ ), also commonly called characteristic impedance, that relates to the stiffness of the proximal aorta or pulmonary artery; a lumped arterial resistance ( $R_a$ ); and a resistance to return of blood from the  $C_v$  to the heart ( $R_v$ ), which is similar, although not identical, to Guyton's resistance to venous return (11). The heart valves permit flow in only one direction through the circuit.

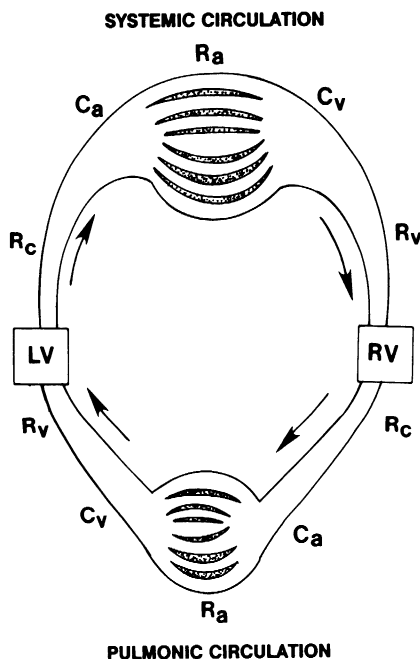


Fig. 1. Schematic representation of simulation used for the analysis. Details of this model are presented in APPENDIX A. RV and LV, right and left ventricles, respectively;  $C_a$  and  $C_v$ , lumped arterial and venous capacitances, respectively;  $R_c$ , proximal characteristic resistance;  $R_a$ , lumped arterial resistance;  $R_v$ , resistance to return of blood from venous capacitance to heart. See text for further details.

The blood volume contained within each of the capacitive compartments is divided functionally into two pools: the unstressed ( $V_U$ ) and the stressed blood volume ( $V_S$ ).  $V_U$ , sometimes referred to as the dead volume, is defined as the maximum volume of blood that can be placed within a capacitive vessel without raising its pressure above 0 mmHg. The blood volume within the capacitive compartment in excess of  $V_U$  is called  $V_S$ . The pressure within the compartment is assumed to rise linearly with  $V_S$  in relation to the compliance ( $C$ ):  $P = V_S/C$ . The unstressed volume of the entire vascular system is equal to the sum of  $V_U$  of all the capacitive compartments; similarly, the total body stressed volume equals the sum of  $V_S$  for all compartments.

The normal value of each parameter of the model was set to be appropriate for a 70–75 kg man (body surface area 1.9 m<sup>2</sup>). These values, adapted from values in the literature (16, 17, 28, 31, 32), are listed in Table 1. Baseline cardiovascular performance indexes obtained from the simulation using these normal parameter values are shown in Table 2.

**Protocols.** Several analyses were carried out to determine how cardiac output (CO), mean arterial pressure (MAP), and pulmonary venous pressure (PVP, which was equated with pulmonary capillary pressure), change in response to variations in specific cardiovascular parameters. The impact of reduced ventricular strength on cardiovascular performance was tested by simulating acute global ventricular dysfunction by progressively decreasing the value of  $E_{es}$ . To test whether the conclusions drawn from this analysis were dependent on the way ventricular performance was depressed, we also simulated acute regional myocardial infarction using a model validated in animal studies (36). After exploring the direct hemodynamic consequences of decreased ventricular contractile strength, the impact of increased  $R_a$ , heart rate, and changes in the distribution of blood volume between the stressed and unstressed pool were tested separately and then in combination. Finally, the heart model was modified so as to include the influence of the pericardium. The details of the pericardial model are provided in APPENDIX B.

## RESULTS

**Impact of decreased LV contractility.** The purpose of the first analysis was to determine the hemodynamic re-

Table 1. Baseline parameter values chosen to be appropriate for 75 kg man

Heart parameters	RV	LV
End-systolic elastance ( $E_{es}$ ), mmHg/ml	0.7	3.0
Unstressed volume ( $V_0$ ), ml	0	0
Time to end systole ( $T_{es}$ ), ms	175	175
Time constant of relaxation ( $\tau$ ), ms	25	25
Scaling factor for EDPVR ( $A$ ), mmHg	0.35	0.35
Exponent for EDPVR ( $B$ ), ml <sup>-1</sup>	0.023	0.033
Circulation parameters	Pul	Sys
Arterial resistance ( $R_a$ ), dyn · s · cm <sup>-5</sup>	40	1,200
Characteristic resistance ( $R_c$ ), dyn · s · cm <sup>-5</sup>	27	40
Venous resistance ( $R_v$ ), dyn · s · cm <sup>-5</sup>	20	20
Total resistance ( $R_T$ ), dyn · s · cm <sup>-5</sup>	87	1,260
Arterial capacitance ( $C_a$ ), ml/mmHg	13	1.32
Venous capacitance ( $C_v$ ), ml/mmHg	8	70
Common parameters		
Heart rate (HR), beats/min		75
Total blood volume ( $V_T$ ), ml		5,500
Total stressed blood volume ( $V_S$ ), ml		750
Total unstressed blood volume ( $V_U$ ), ml		4,750

RV and LV, right and left ventricles; EDPVR, end-diastolic pressure-volume relation; Pul and Sys, pulmonary and systemic circulation, respectively. Values adapted from literature.

Table 2. Cardiovascular performance indexes derived from model with normal parameter values

Aortic pressure, mmHg	115/61 (mean 86)
Pulmonary pressure, mmHg	30/12 (mean 16)
Cardiac output, l/min	5.4
Left ventricular	
P, mmHg	115/12
V <sub>ed</sub> , ml	106
SV, ml	70.8
EF, %	67
Right ventricular	
P, mmHg	30/2
V <sub>ed</sub> , ml	95.2
SV, ml	70.8
EF, %	75

P, ventricular pressure; V<sub>ed</sub>, end-diastolic volume; SV, stroke volume; EF, ejection fraction.

sponses to a primary decrease in LV contractile strength in the absence of other changes in cardiovascular properties. Results are shown in Fig. 2. As  $E_{es}$  was decreased from a control value of 3 (vertical line on graph) to 1 mmHg/ml, corresponding to a severe reduction in contractile performance, there was a prominent decrease in CO and MAP. The important finding, however, was that PVP increased from the control value of 12 to only 16 mmHg. Thus pulmonary congestion could not be created in this model simply by inducing a profound reduction in LV strength.

To test whether this result was dependent on the way in which ventricular contractile strength was reduced, the impact of simulated acute myocardial infarction on LV filling pressure was determined. The results, presented in Fig. 3, show that as the percent of the myocardium rendered ischemic is increased from 0 to 50%, there are physiologically profound decreases in CO and MAP; however, PVP increased from the baseline value to only 18 mmHg. Thus the result that PVP does not increase significantly with a large decrease in LV pumping ability appears to be independent of the way LV chamber strength is decreased.

In addition, it is commonly known that diastolic function is impaired during ischemia (21), and this can cause changes in the rate and extent of myocardial relaxation. To test whether such changes would modify the findings,  $\tau$  was increased from its baseline value of 25 to 125 ms while LV  $E_{es}$  was at its reduced value of 1.5 mmHg/ml. In

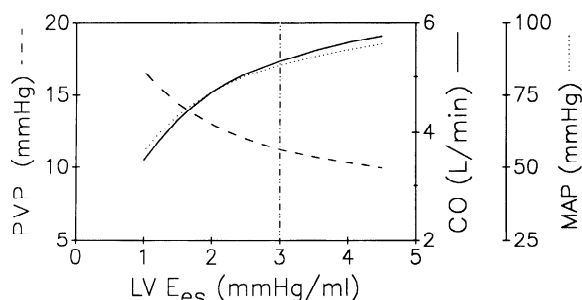


Fig. 2. Impact of changing LV end-systolic elastance ( $E_{es}$ ) on hemodynamic indexes in absence of changes in other cardiovascular parameters. While cardiac output (CO) and mean arterial pressure (MAP) decrease significantly as LV  $E_{es}$  was decreased from its control value (shown by vertical dash-dot line), pulmonary venous pressure (PVP) increased by only a very small amount.

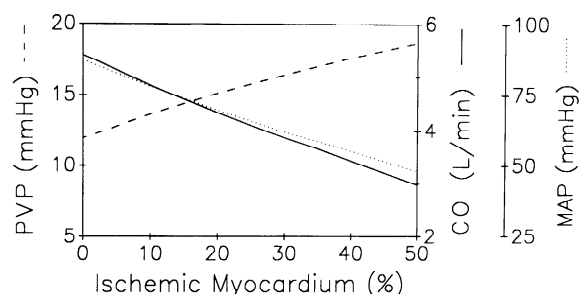


Fig. 3. Impact of simulated acute myocardial infarction on hemodynamic indexes. As percent of ventricle rendered ischemic increases, CO and MAP decrease but PVP increases only by a small amount.

response to this dramatic change in  $\tau$ ,  $P_{ed}$  varied  $<1$  mmHg from the starting value and was nearly unchanged at 14 mmHg, while LV  $V_{ed}$  decreased minimally from 113 to 104 ml. Next, with  $\tau$  set at 50 ms and LV  $E_{es}$  at 1.5 mmHg/ml, we increased the diastolic stiffness of the ventricle by increasing the value of LV  $B$  (the exponent of the diastolic PV relation; see Table 1) from its baseline value of 0.033 to 0.044 ml<sup>-1</sup> (a 33% increase). This represents a very large increase in LV stiffness: for instance, the pressure on the end-diastolic pressure-volume relation (EDPVR) at a volume of 110 ml increased from 14 to 38 mmHg. In response to this dramatic increase in LV diastolic stiffness, LV  $P_{ed}$  increased from 14 to only 17 mmHg while LV  $V_{ed}$  decreased markedly from 112 to 91 ml. Thus changes in the rate or extent of relaxation did not alter the major finding that PVP does not rise as a direct hemodynamic consequence of impaired ventricular function, systolic or diastolic.

**Impact of increasing systemic resistance.** To test the role of increasing systemic  $R_a$  in the generation of pulmonary edema, LV  $E_{es}$  was set at one-half normal (1.5 mmHg/ml), and systemic  $R_a$  was increased from its control value of 1,200 to 6,700 dyn·s·cm<sup>-5</sup>, a much greater change than observed typically in the clinical setting; note that for this analysis,  $R_c$  was fixed at its control value of 40 dyn·s·cm<sup>-5</sup>. The results are shown in Fig. 4; the vertical line indicates the normal  $R_a$  value. As  $R_a$  was increased, CO decreased and MAP increased, while PVP changed very little. Thus the increase in  $R_a$  that accompanies acute ventricular failure may effectively serve to increase blood pressure but has a deleterious effect on CO;

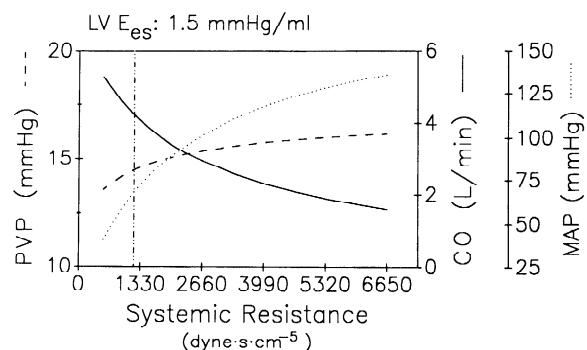


Fig. 4. Impact of increasing total systemic resistance on cardiovascular performance with LV  $E_{es}$  set at one-half its control value. As resistance is increased from its control value (shown by vertical dash-dot line) CO decreases and MAP increases, but PVP is relatively unaffected.

increasing  $R_a$  did not cause a significant rise in PVP during acute heart failure in this model.

Further analysis showed that changes in pulmonic  $R_a$ , either alone or in combination with changes in systemic  $R_a$ , did not modify the conclusion that PVP was relatively insensitive to marked elevations in systemic  $R_a$ .

**Impact of increasing heart rate.** The role of increasing heart rate to a maximum of 180 beats/min on cardiovascular performance with LV  $E_{es}$  set at one-half normal (1.5 mmHg/ml) is illustrated in Fig. 5. For this analysis  $T_{es}$  and  $\tau$  were also decreased as heart rate was increased. CO increased substantially up to a heart rate of 120 beats/min, after which it plateaued and then declined. This nonlinear behavior reflects the balance between increasing CO secondary to increased beat frequency and decreasing stroke volume secondary to decreased LV filling. MAP tracks CO output because, in this analysis, peripheral resistance is fixed. PVP decreased as heart rate was increased. Also shown in this plot is LV  $P_{ed}$ , which is ordinarily equal to PVP; at high heart rates, however, filling is curtailed and LV  $P_{ed}$  falls slightly below PVP.

The precise nature of each of the curves shown in Fig. 5 is highly dependent on the parameters of the EDPVR,  $\tau$  and  $R_v$ . Extensive analysis, however, failed to identify any combination of these parameter values that could cause an increase in PVP with increases in heart rate. In particular, even if  $\tau$  were increased instead of decreased with the heart rate changes, PVP did not rise; rather, in such a case LV  $V_{ed}$  decreased so that PVP was relatively unaffected (see DISCUSSION for further explanations).

**Impact of changing stressed vascular volume.** Sympathetic stimulation increases the  $V_S$  by decreasing  $V_U$  of the splenic, hepatic, and systemic venous beds. In the acute setting, total blood volume is nearly constant, so that a decrease in  $V_U$  would be accompanied by an approximately equal increase in  $V_S$ . It is known, however, that when venous pressure rises, fluid can shift from the intravascular space to the extravascular space (1, 20), and therefore this assumption may be only an approximation. More recent studies have suggested that the magnitude of this effect is small under normal conditions (33), and therefore in the present analysis the sum of  $V_U$  and  $V_S$  will be assumed to be a constant.

The hemodynamic impact of decreasing total body  $V_U$  from the control value of 4,750 (vertical line) to 3,850 ml

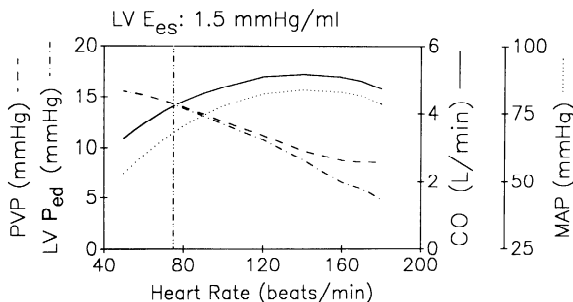


Fig. 5. Impact of increasing heart rate on cardiovascular performance with LV  $E_{es}$  set at one-half its control value. As heart rate is increased from its control value (shown by vertical dash-dot line) CO and MAP increase and then plateau and finally decrease at very high heart rates. PVP decreases continuously with heart rate. LV end-diastolic pressure ( $P_{ed}$ ), which normally equals PVP in the simulation, becomes less than PVP by a small amount as heart rate is increased above 120 beats/min.

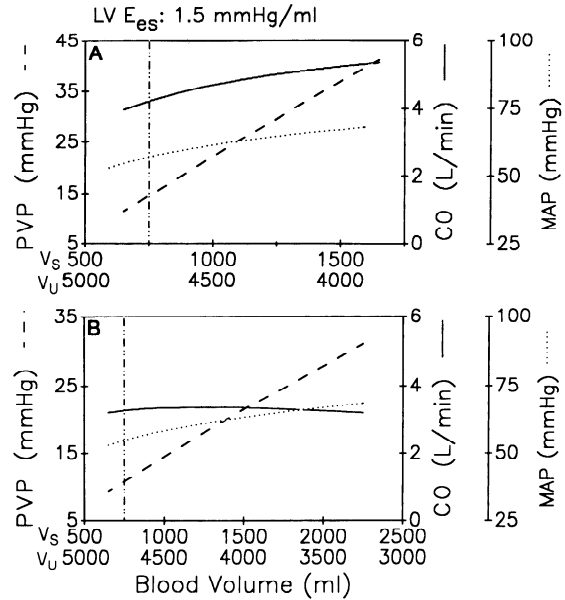


Fig. 6. Impact of decreasing unstressed vascular volume ( $V_U$ ) with complementary increases in stressed vascular volume ( $V_S$ ) on cardiovascular performance with  $E_{es}$  set at one-half its control value. When no pericardium is present (A), PVP rises substantially as  $V_S$  is increased from its control value (shown by vertical dash-dot line); this is accompanied by modest increases in MAP and CO. In presence of pericardium (B), responses of CO and MAP to changes in  $V_S$  are blunted, but PVP still increases substantially.

with LV  $E_{es}$  set at one-half normal is shown in Fig. 6A. Note that concomitant with this 20% change in  $V_U$ ,  $V_S$  is increased by over 100% (from 750 to 1,650 ml). With this change, CO and MAP increased substantially. The significant finding, however, is that this is the only intervention tested that leads to a substantial increase in PVP. PVP reached 25 mmHg when  $V_U$  had fallen to  $\sim$ 4,400 ml, a decrease of only 7% from the control value; it is important to recognize that accompanying this seemingly small decrease in  $V_U$ ,  $V_S$  has risen from 725 to 1,100 ml, an increase of nearly 50%.

**Impact of pericardium.** In the simulation used thus far, right and left ventricular properties were independent of each other. In reality, right and left ventricular properties are interdependent because they share a common wall, the septum, and because they are encased within a single sack, the pericardium. The impact of septum-mediated ventricular interaction has been analyzed in detail previously (29). The results of that analysis suggested that for equivalent net chamber properties, changes in CO resulting from decreases in ventricular strength are not significantly different if the heart is modeled as two interacting chambers or as two independent chambers; therefore, further analysis of this form of interaction will not be presented here.

Pericardial constraints, modeled as detailed in APPENDIX B, have the effect of increasing right and left ventricular pressures at any given volume by an amount that is nonlinearly related to the sum of right and left ventricular volumes. The impact of this constraint on the overall cardiovascular response to increased  $V_S$  is summarized in Fig. 6B. As shown, for similar changes in  $V_S$  and  $V_U$ , the pericardium attenuated the increases in CO

and MAP while lessening the rise in PVP to a small degree.

The pericardium also had a profound effect on central venous pressure (CVP) (not shown graphically). As  $V_U$  was decreased from 4,750 to 3,850 ml, CVP increased from 1.1 to 3.2 mmHg in the absence of the pericardium; in the presence of pericardial constraints, CVP changed from 3.4 mmHg at baseline to 13.5 mmHg after the shift in  $V_U$ . Thus, in this model, pericardial constraints are required to predict elevations in CVP, which commonly occur in patients with acute LVD in the absence of right ventricular dysfunction.

*Impact of sympathetic activation and pericardium on overall hemodynamic response to acute LVD.* To further illustrate the important role of the pericardium and sympathetic activation in determining overall hemodynamic status, we obtained pressure-volume (PV) loops from the computer simulation under various conditions (see Fig. 7). The dotted lines show the ventricular EDPVR and the end-systolic pressure-volume relation (ESPVR) as labeled. The PV loop shown by the dashed line was obtained with no pericardial constraints and with model parameters set at control values except for  $E_{es}$ , which was set at one-half its control value. Note the very low peak ventricular pressure (equal to systolic blood pressure) and relatively low  $P_{ed}$  (bottom right corner of loop). Under these conditions stroke volume was  $\sim 50$  ml and CO was only 3.9 l/min at the control heart rate of 75 beats/min. The dashed-dotted line shows the PV loops resulting when sympathetic activation is simulated by increasing  $R_a$  to 2,500  $\text{dyn}\cdot\text{s}\cdot\text{cm}^{-5}$ , increasing heart rate to 125 beats/min, and increasing  $V_S$  to 1,950 ml (still without pericardial constraints). Note the marked increase in LV  $P_{ed}$  to 38 mmHg and peak LVP to  $\sim 170$  mmHg; while stroke volume was decreased to 32 ml, CO increased to 4.3 l/min because of the high heart rate. When pericardial effects are introduced (solid line), the bottom portion of the PV loop becomes substantially elevated above the

EDPVR, the  $V_{ed}$  decreases, and LV  $P_{ed}$  decreased by a small amount; as a consequence, stroke volume fell to 26 ml, CO fell to 3.4 l/min, and peak LV pressure dropped a small amount. Thus, as noted above, the pericardial constraints attenuated the beneficial hemodynamic effects of increased  $V_S$ .

The CVP corresponding to the dashed-dotted PV loop in Fig. 7 (no pericardium) was only 2 mmHg, essentially the baseline value. However, when the pericardium was added, CVP increased to 12 mmHg, again suggesting a mechanism for why CVP increases when there is acute LVD in the absence of right ventricular dysfunction.

In summary, this model predicts a hemodynamic state that is commonly encountered in patients presenting with acute pulmonary edema secondary to many causes in whom ventricular dysfunction is not severe enough to induce shock. Specifically, the model predicts an elevated MAP, elevated PVP and CVP, and decreased CO in the presence of tachycardia.

## DISCUSSION

The results of this theoretical analysis suggest that significant elevations of PVP do not occur as a direct hemodynamic consequence of acute LVD. Pure decreases in LV strength were associated with marked decreases in blood pressure and cardiac output but only minimal elevations in PVP. Simulated, stepwise activation of autonomic reflex components was quite revealing as to the role of individual compensatory mechanisms in both normalizing and worsening overall hemodynamic status after the onset of LVD. Increases in peripheral resistance effectively increased blood pressure but caused further decreases in cardiac output. Increases in heart rate acted to restore cardiac output. However, PVP did not rise appreciably in response to either of these interventions. The only maneuver that caused significant elevation of PVP in the simulation was an increase in the stressed blood volume. Because, under normal conditions, unstressed blood volume accounts for as much as 85% of the total volume, shifts of as little as 15% of this pool into the stressed pool caused tremendous increases in PVP. However, the hemodynamic benefits of such an increase (improving blood pressure or cardiac output) are overshadowed by its detrimental effects of causing pulmonary congestion. Simulation of pericardial constraints are predicted to markedly attenuate the beneficial effects of increased stressed vascular volume, although not to appreciably alter the concomitant pulmonary vascular congestion.

The results of this analysis emphasize that with acute LVD, ventricular filling pressure may predominantly be determined by the vascular system, and not the other way around. This is opposite to the commonly held notion that impaired LV function leads to a primary increase in ventricular  $P_{ed}$  that is transmitted backward to the pulmonary venous system. It is also opposite to the frequently held notion that impaired LV function leads to a primary increase in PVP due to shifts of blood from systemic to pulmonic system, which are purely on the basis of a transient mismatch in right and left ventricular cardiac output. In contrast, according to the currently pro-

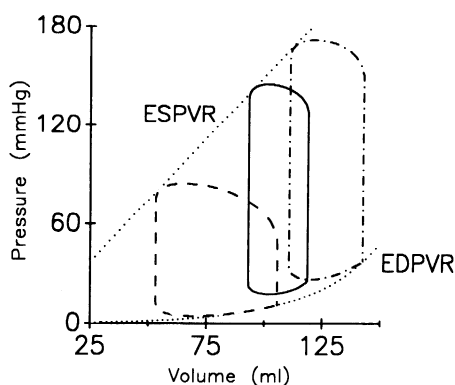


Fig. 7. PV loops illustrating dramatic impact of pericardium on simulated hemodynamic responses to sympathetic activation. Dotted lines, end-systolic and end-diastolic pressure-volume relations (ESPVR and EDPVR, respectively). Dashed line, PV loop obtained with  $E_{es}$  set at one-half control value but other cardiovascular parameters fixed at their control value. Heart rate was increased to 135 beats/min,  $R_a$  was increased to 2,900  $\text{dyn}\cdot\text{s}\cdot\text{cm}^{-5}$ , and  $V_S$  was increased to 1,950 ml. In absence of pericardium (dash-dot line), PV loop shifts to right [increase in end-diastolic volume ( $V_{ed}$ )]. However, in presence of pericardium (solid line), PV loop shifts upward off the EDPVR. As a result of curtailed increase in  $V_{ed}$ , stroke volume is smaller and peak pressure is less than that observed in absence of pericardium.

posed scheme, the increases in PVP and LV filling pressure are both mediated by central nervous system actions (venoconstriction); that is, the diastolic LV is a passive element that responds to the external forces imposed on it by the vascular system.

*Relation to previous work.* Current understanding of the dynamics of the closed-loop circulatory system is largely based on the pioneering theoretical and experimental work of Guyton and his colleagues (10). They (13) and others (22) have examined changes in the venous return curve (the relation between right atrial pressure and rate of venous return) during acute heart failure. These studies revealed that during acute heart failure the venous return curve shifts downward and to the left (i.e., less venous return for a given right atrial pressure), and this has been attributed to shifting of blood from the systemic to pulmonic circuit. It has been assumed that these shifts result directly from a transient mismatch between right and left ventricular stroke volumes that occurs over the first several seconds after an insult to LV function. While accumulation of blood in the pulmonic circuit, which is also predicted by the current analysis, must result from transient mismatches between right and left ventricular stroke volumes, the underlying mechanism suggested by the present analysis is very different than that assumed by Guyton. As indicated above, Guyton and colleagues (9) assumed that the transient stroke volume mismatch was a direct consequence of the abruptly decreased LV pumping ability; the present analysis suggests that this does not occur (Fig. 2; no significant shift in blood in the absence of venoconstriction). In contrast, the present analysis suggests that the fluid accumulation in the lung is due first to functional redistribution of blood from unstressed to stressed circulating pool. Second, for the case that this functional redistribution of blood occurs mostly on the basis of splanchnic venoconstriction (see below), a transient increase in right ventricular stroke volume will result from the consequent increase in central venous pressure. The recruited fluid will ultimately distribute throughout the circulatory system; the amount of fluid ultimately settling in the lung will depend on the equilibrium flow through the circuit and the relative compliances of the various vascular beds.

One additional limitation of these previous studies and theories is failure to account for the effects of the pericardium in understanding closed-loop cardiovascular dynamics. It is interesting that in the earlier theory (9) central venous pressures did not rise with pure LVD. This is also a common experience in experimental settings when the pericardium is removed (22). However, rises in central venous pressure are common in patients who present with acute pulmonary edema; the present theory suggests that this finding is due to pericardial constraints; changes in venous tone in and of themselves do not appear to be adequate to explain this finding.

*Evidence for shifts of vascular capacity.* It has long been recognized that sympathetic nervous system activation leads to decreased systemic vascular capacity. This is brought about predominately by changes in the splanchnic vascular bed that result in leftward shift of the venous pressure-volume relation (2-6, 8, 26, 32).

Evidence that decreased vascular capacity plays an important role in the development of acute pulmonary edema has been provided by recent studies in an ischemic model of LVD in intact dogs (30, 39). Microsphere embolization of the coronary artery bed resulted in significant increases in pulmonary capillary pressures associated with ~15-20% decreases in the volume-axis intercept of the whole gut venous pressure-volume relation. Of note, there was no significant change in the slope of these venous relations, indicating that the compliance of the vascular bed was unchanged. It was also shown that these shifts were reversed by either nitroglycerin (30) or Enalaprilat (40) administration.

Evidence for sympathetic modulation of vascular capacity in humans has also been provided recently by Robinson et al. (24) in subjects with no known cardiac disease. When subjected to mental stress, the venous pressure-volume relation of the forearm shifted to the left in a parallel manner, with the volume-axis intercept decreasing by ~14%.

There is recent evidence that parallel leftward shifts in the venous pressure-volume curve, such as have been observed during acute heart failure, also occur and are sustained in an experimental model of chronic heart failure (18). Furthermore, these curves shift back toward normal when ventricular function is allowed to recover. Thus, if the results of the present analysis are momentarily extended to chronic heart failure, it can be hypothesized that changes in venous tone could play a pivotal role in determining ventricular filling pressures in chronic heart failure.

Measurements to confirm that shifts occur in the venous pressure-volume relations in human subjects in the throws of an acute bout of pulmonary edema have not been made. Nevertheless, peripheral autonomic blockade has long been recognized to decrease central venous pressure in patients with chronic heart failure, and this effect was hypothesized to be related in part to venodilatation (23).

*Potential role of atria.* The present simulation did not include effects of the atria. Atrial contraction enhances ventricular filling so that ventricular  $P_{ed}$  may be higher than PVP at low heart rates and can more nearly reach PVP at high heart rates. In addition, model analysis has indicated that the compliance of the atrial chamber facilitates transfer of blood from the veins to the ventricle (35). However, because of the impact of pericardial constraints, even relatively substantial increases in LV filling pressure would be ineffective at increasing ventricular diastolic volume. Thus it is anticipated that the impact of atria on enhancing cardiac output or lessening the degree of pulmonary vascular congestion would be minimal.

Furthermore, pericardial pressures are determined not only by ventricular volumes but by the sum of the volumes of all four cardiac chambers (12, 15). In fact, the atria have been shown to have relatively profound influences on pericardial pressures. It would be expected, therefore, that had atria been included in the simulation, the pericardial constraints would have been exaggerated compared with those presented in Figs. 6 and 7.

*Physiology of venodilator therapy in acute pulmonary*

*edema.* Traditional treatment of acute pulmonary edema includes administration of diuretics, nitrates, and morphine. These agents act to decrease intravascular volume and/or to increase venous capacity, thus reducing stressed blood volume; both of these effects lead to a decrease in LV filling pressure. Decreases in LV  $P_{ed}$  would ordinarily lead to decreases in LV  $V_{ed}$  and thus decreases in cardiac output via the Frank-Starling mechanism. However, these therapies are known to increase, not decrease, cardiac output. How is it, then, that a treatment that leads to a decrease in ventricular preload pressure also leads to an increase in cardiac output? One factor may be that decreases in PVP will result in improved blood oxygenation, which, in turn, may enhance ventricular performance. However, further model analysis supports a previously proposed hemodynamic mechanism for the beneficial effects of venodilators in heart failure, which involves the pericardium (14, 25, 37, 38). As PVP is decreased, biventricular diastolic pressures decrease with an easing of pericardial pressures; that is, diastolic ventricular pressures fall as a result of decreased pericardial pressures but ventricular volumes do not decrease appreciably. As a specific example, consider the effect of reducing stressed blood volume in the computer model (i.e., to simulate venodilator therapy) starting from conditions considered representative of those accompanying acute LVD shown by the pressure-volume loop drawn with the solid line in Fig. 7. This pressure-volume loop has been redrawn in Fig. 8, again with a solid line (note expanded scales). When we start from the specified conditions (with pericardial constraints present),  $V_S$  was decreased from 1,950 to 1,250 ml, simulating a rather large decrease in stressed volume. After this, LV diastolic pressure decreased substantially from 29 to 18 mmHg, but LV  $V_{ed}$  only decreased from 118 to 111 ml and cardiac output from 3.4 to 3.3 l/min. According to the Frank-Starling mechanism, the strength of ventricular contraction is determined by the  $V_{ed}$ . Thus stroke volume can be maintained in the face of venodilatation because the pressure-volume loop shifts downward, instead of shifting leftward, as a result of pericardial-ventricular interactions. Additional hemodynamic benefits would be expected from the actions of these agents as mild afterload reducers, which would allow cardiac output to increase above the starting value and thus explain the clinical scenario.

The results of this theoretical analysis are also consistent with previous clinical findings indicating that, while increasing cardiac output, treatment of heart failure with an agent that is primarily an afterload reducer does not relieve pulmonary congestion (7). The analysis specifically indicates that changes in afterload resistance have very little effect on pulmonary venous pressure (Fig. 4). Because the analysis indicates that the primary factor responsible for increasing pulmonary pressure is changes in venous capacity, it follows that impacting on that part of the system would be the most effective in alleviating the problem.

*Role of sympathetic nervous system in heart failure.* As reviewed by Packer (19) recently, the prevailing view of the cardiology community regarding whether the auto-

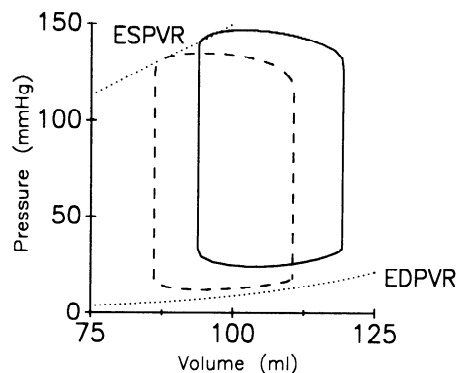


Fig. 8. Simulated effect of venodilator therapy. Solid line, PV loop expected in patient with acute LV dysfunction after activation of sympathetic system (see legend of Fig. 8 for hemodynamic parameters). Stressed vascular volume is then decreased from starting value of 1,950 to 1,250 ml to simulate effects of pure venodilator. The resulting PV loop (dashed line) shifts downward back to EDPVR and slightly to left.  $P_{ed}$  drops substantially from 30 to 18 mmHg, while  $V_{ed}$  decreases only a small amount from 118 to 111 ml because of pericardial constraints. Since  $V_{ed}$  changes little, stroke volume can be maintained despite a large drop in  $P_{ed}$ .

nomous nervous system acts to improve or worsen the symptoms of heart failure has shifted several times over the past 50 years. For the most part, however, these arguments have dealt with chronic heart failure in which factors other than those considered in the present analysis play important roles. These include, but are not limited to, salt and water retention, ventricular and pericardial remodeling, and other consequences of chronically elevated concentrations of a multitude of neural and hormonal substances (e.g., catecholamines, renin, atrial natriuretic hormone). However, discussion of the role of the sympathetic nervous system in the development of acute heart failure has received less attention.

It has been hypothesized that the sympathetic nervous system evolved in large part to allow animals to deal with episodes of stress such as occurs with acute hemorrhage. In the case of an acute hemorrhage in an otherwise young, healthy individual, shifts of volume from the unstressed to the stressed blood pool could serve as a powerful way of compensating for quantities of lost blood (8). The other major accompanying autonomic actions (i.e., increased arterial resistance, heart rate, and ventricular contractility) serve appropriately to restore cardiac output and blood pressure. In such a situation, the centrally orchestrated alterations of the individual components of the otherwise healthy cardiovascular system act in concert to normalize hemodynamic status. While the stimuli that trigger autonomic activation with acute heart failure are similar to those of acute stress (i.e., decreased blood pressure and cardiac output), it is apparent that the optimal hemodynamic remedy is not the same. Specifically, the results of the present analysis indicate that recruitment of blood volume is detrimental to the organism as a whole. Accordingly, it can be argued that the autonomic system is not designed to deal optimally with the hemodynamic state created by failing ventricular pump function.

*Limitations.* In the present study, a relatively simple model of the cardiovascular system has been analyzed. Care has been taken in selecting parameter values. Furthermore, many additional analyses have been performed

using a wide range of parameter values and combinations of parameter values to ensure that the main conclusion of this study is not peculiar to one narrow range of parameter values. Nevertheless, the results and conclusions should be viewed as theoretical and subject to experimental verification (see below for further discussion). Generally, the model behaved in a manner consistent with clinical and experimental observations in almost every way. An exception to this was one of the effects of pericardial constraints. In the model, when pericardial restraints are abruptly removed, LV diastolic pressure increases slightly. It is generally recognized that when the pericardium is removed from the heart, LV diastolic pressure decreases. The reason that LV diastolic pressures rise in the simulation is that when pericardial constraints are removed there is a marked decrease in right ventricular (RV) diastolic pressure; in response to this there is enhanced filling of the RV and an increased RV stroke volume (with RV greater than LV stroke volume) that persists until a new equilibrium state is established. As a result of this, there is a redistribution of fluid from the systemic venous capacitance to the pulmonary venous capacitance, with concomitant increase in LV  $P_{ed}$ . Whether this represents a point of divergence between the model predictions and reality is not certain because an experiment in which heart failure has been created with an intact pericardium and blocked autonomic reflexes followed by pericardiectomy has not been performed.

One additional assumption in the model deserves further mention. We have assumed that total blood volume remains constant after venoconstriction. However, as pointed out above, fluid can shift from the intravascular to extravascular space when venous pressure rises; it has been argued that the degree to which this effect can alter blood volume is small (33), although there is some controversy (1, 20). However, this factor is important because one example of this phenomenon is transudation of fluid into the lung interstitial space (and then into the alveoli), which limits oxygen transfer and is likely responsible for some of the symptoms of acute heart failure. Such fluid shifts would cause any increase in  $V_S$  to be less than the initiating decrease in  $V_U$ . The consequence of venoconstriction that was determined to cause the increase in pulmonary pressures was the increase in  $V_S$ ; therefore, intravascular-to-extravascular fluid shifts would have the effect of attenuating the effect of venoconstriction to increase venous pressures. It is important to note, therefore, that this effect does not alter the conclusions of this theoretical study in any way; it merely indicates that greater decreases in  $V_S$  are required to cause a given change in  $V_U$ .

**Conclusions.** The conclusions of this study are derived from model analysis and not directly from experimental observations. With regard to the role of such models in cardiovascular research, Milnor wrote:

Fundamentally, they serve to put an hypothesis into concise quantitative form, which has the peripheral benefit of forcing an investigator to make his ideas free of ambiguity. . . . Once a mathematical or analogue model has been completed, it can be used to compute the effects of changing any parameter, often with results that were not obvious

before. At that point there is a strong temptation to believe that the results reveal something about the circulation in vivo, which they do not. What they tell us are the implications of the hypotheses built into the model, hypotheses that may or may not be valid in living animals. Models are thus a kind of temporary assembly of working assumptions, and their purpose should be to provoke, not take the place of, new experimental observations. (16, p. 98)

In choosing to use analytic methods to explore the hemodynamics of heart failure, we have been forced to clarify and specify our ideas about cardiovascular mechanics. We have quantitatively linked basic concepts of hemodynamics, pericardial physiology, and reflex-mediated changes in cardiovascular parameters. Consequently, the results support a comprehensive theory that explains why pulmonary congestion and elevations of central venous pressure occur after the onset of acute LVD; the theory also provides an explanation for time-honored treatments of this condition. The results should not be viewed quantitatively but rather in a qualitative sense with regard to how we think of the pathophysiology of acute heart failure. Hopefully, in revealing inconsistencies between current theories and clinical observations, new discussions and experimentation will be provoked that will help advance our understanding and treatment of heart failure.

#### APPENDIX A

The equations describing the model depicted in Fig. 1 are reviewed in this section. The ventricles were modeled as time-varying elastances with linear end-systolic and nonlinear end-diastolic pressure-volume relations. Left ventricular pressures ( $P_{LV}$ ) and volume ( $V_{LV}$ ) were interrelated by the following equations, which have been used before (29)

$$P_{LV}(t) = [P_{es,LV}(V_{LV}) - P_{ed,LV}(V_{LV})]\epsilon_{LV}(t) + P_{ed,LV}(V_{LV}) \quad (A1)$$

where

$$\epsilon_{LV}(t) = \frac{1}{2} \left[ \sin \left( \frac{\pi}{T_{es}} t - \frac{\pi}{2} \right) + 1 \right] \quad \text{for } t < \frac{3T_{es}}{2} \quad (A2)$$

$$\epsilon_{LV}(t) = 0.5 \exp[(t - 3T_{es}/2)/\tau] \quad \text{for } t \geq 3T_{es}/2 \quad (A3)$$

$$P_{es,LV}(V_{LV}) = E_{es,LV}(V_{LV} - V_{0,LV}) \quad (A4)$$

$$P_{ed,LV}(V_{LV}) = A_{LV} \{ \exp[B_{LV}(V_{LV} - V_{0,LV})] - 1 \} \quad (A5)$$

A comparable set of equations was used to describe RV function; all of the parameters describing RV and LV function were independent of each other except for  $T_{es}$  and  $\tau$ , which were set at the same values for both ventricles; thus  $\epsilon_{LV}(t)$  and  $\epsilon_{RV}(t)$  were identical functions.

The capacitance of the systemic circulation was divided into arterial and venous capacitances,  $C_{a,s}$  and  $C_{v,s}$ , respectively. Similarly, the pulmonary circulation had arterial and venous capacitive elements,  $C_{a,p}$  and  $C_{v,p}$ , respectively. Pressures (P) and volumes (V) in each capacitance were related by the following linear relations

$$P_{C_{a,s}} = V_{C_{a,s}}/C_{a,s} \quad (A6)$$

$$P_{C_{v,s}} = V_{C_{v,s}}/C_{v,s} \quad (A7)$$

$$P_{C_{a,p}} = V_{C_{a,p}}/C_{a,p} \quad (A8)$$

$$P_{C_{v,p}} = V_{C_{v,p}}/C_{v,p} \quad (A9)$$

In each of these equations, the volume represents the stressed volume in the capacitance. The total unstressed volume of the system equals the sum of the unstressed volumes of all four capacitances. Therefore, total unstressed volume could be considered as a single parameter ( $V_U$ ), without the need to be broken down into unstressed volumes of individual compartments. Therefore, total body blood volume ( $V_T$ ), unstressed volume, and volumes on individual capacitances are interrelated by

$$V_T = V_{C_{a,s}} + V_{C_{v,s}} + V_{C_{a,p}} + V_{C_{v,p}} + V_U + V_{LV} + V_{RV} \quad (A10)$$

A set of six differential equations described changes in volumes in the four capacitors and the two ventricles as functions of time in terms of the pressure across each element and the value of the resistance connecting between different elements (see Table 1 and Fig. 1 for abbreviations; subscripts s and p denote systemic and pulmonary, respectively)

$$\frac{dV_{LV}(t)}{dt} = \frac{P_{C_{v,p}}(t) - P_{LV}(t, V_{LV})}{R_{v,p}} \alpha_{LV} - \frac{P_{LV}(t, V_{LV}) - P_{C_{a,s}}(t)}{R_{c,s}} \beta_{LV} \quad (A11)$$

$$\frac{dV_{C_{a,s}}(t)}{dt} = \frac{P_{LV}(t, V_{LV}) - P_{C_{a,s}}(t)}{R_{c,s}} \beta_{LV} - \frac{P_{C_{a,s}}(t) - P_{C_{v,s}}(t)}{R_{a,s}} \quad (A12)$$

$$\frac{dV_{C_{v,s}}(t)}{dt} = \frac{P_{C_{a,s}}(t) - P_{C_{v,s}}(t)}{R_{a,s}} - \frac{P_{C_{v,s}}(t) - P_{RV}(t, V_{RV})}{R_{v,s}} \alpha_{RV} \quad (A13)$$

$$\frac{dV_{RV}(t)}{dt} = \frac{P_{C_{v,s}}(t) - P_{RV}(t)}{R_{v,p}} \alpha_{RV} - \frac{P_{RV}(t, V_{RV}) - P_{C_{a,p}}(t)}{R_{c,p}} \beta_{RV} \quad (A14)$$

$$\frac{dV_{C_{a,p}}(t)}{dt} = \frac{P_{RV}(t, V_{RV}) - P_{C_{a,p}}(t)}{R_{c,p}} \beta_{RV} - \frac{P_{C_{a,p}}(t) - P_{C_{v,p}}(t)}{R_{a,p}} \quad (A15)$$

$$\frac{dV_{C_{v,p}}(t)}{dt} = \frac{P_{C_{a,p}}(t) - P_{C_{v,p}}(t)}{R_{a,p}} - \frac{P_{C_{v,p}}(t) - P_{LV}(t, V_{LV})}{R_{v,p}} \alpha_{LV} \quad (A16)$$

The values of  $\alpha$  and  $\beta$  in these equations are set at either 0 or 1 depending on whether ventricular filling or ejection are occurring

$$\begin{aligned} \alpha_{LV} &= 1 & \text{if } P_{LV}(t) < P_{C_{v,p}}(t) & \quad \alpha_{RV} = 1 & \text{if } P_{RV}(t) < P_{C_{v,s}}(t) \\ &= 0 & \text{otherwise} & \quad &= 0 & \text{otherwise} \\ \beta_{LV} &= 1 & \text{if } P_{LV}(t) > P_{C_{a,s}}(t) & \quad \beta_{RV} = 1 & \text{if } P_{RV}(t) > P_{C_{a,p}}(t) \\ &= 0 & \text{otherwise} & \quad &= 0 & \text{otherwise} \end{aligned}$$

These simultaneous differential equations were solved using numerical methods.

## APPENDIX B

*Modeling the effects of the pericardium.* Net ventricular pressure at any instant in time in the presence of a pericardium was considered to equal the sum of the ventricular pressure expected for the given ventricular volume and time during the cardiac cycle plus the pressure in the pericardial space (25). Pericardial pressure ( $P_{\text{pericard}}$ ), in turn, was assumed to be equal to a nonlinear function of the sum of instantaneous RV and LV volumes ( $V_{RV}$  and  $V_{LV}$ , respectively)

$$P_{\text{pericard}} = \alpha \exp[\beta(V_{LV} + V_{RV})]$$

The parameter values were chosen to provide a function that

was relatively flat until a critical value at which point pressure rises steeply:  $\alpha = 8.6 \times 10^{-22}$  mmHg;  $\beta = 9.5$  ml<sup>-1</sup>.

Copies of the computer simulation used in this analysis, which run on IBM-compatible computers, along with a basic instruction set (stored in WordPerfect 5.1 format) are available free of charge. Send a blank diskette and stamped self-addressed return envelope to D. Burkhoff, Div. of Circulatory Physiology, Milstein 5-435, Columbia Presbyterian Hospital, 177 Fort Washington Ave., New York, NY 10032.

Address reprint requests to D. Burkhoff.

Received 31 August 1991; accepted in final form 5 April 1993.

## REFERENCES

1. **Ablad, B., and S. Mellander.** Comparative effects of hydralazine, sodium nitrite and acetylcholine on resistance and capacitance blood vessels and capillary filtration in skeletal muscle in the cat. *Acta Physiol. Scand.* 58: 319-329, 1963.
2. **Bennett, T. D., C. F. Wyss, and A. M. Scher.** Changes in vascular capacity in awake dogs in response to carotid sinus occlusion and administration of catecholamines. *Circ. Res.* 55: 440-453, 1984.
3. **Brooksby, G. A., and D. E. Donald.** Dynamic changes in splanchnic blood flow and blood volumes in dogs during activation of sympathetic nerves. *Circ. Res.* 29: 227-238, 1971.
4. **Brunner, M. J., A. A. Shouka, and C. L. Macanespie.** The effect of the carotid sinus baroreceptor reflex on blood flow and volume redistribution in the total systemic vascular bed of the dog. *Circ. Res.* 48: 274-285, 1981.
5. **Carneiro, J. J., and D. E. Donald.** Blood reservoir function of dog spleen, liver, and intestine. *Am. J. Physiol.* 232 (*Heart. Circ. Physiol.* 1): H67-H72, 1977.
6. **Chang, P. I., and D. L. Rutlen.** Effects of  $\beta$ -adrenergic agonists on splanchnic vascular volume and cardiac output. *Am. J. Physiol.* 261 (*Heart. Circ. Physiol.* 30): H1499-H1507, 1991.
7. **Chatterjee, K., W. W. Parmley, B. Massie, B. Greenberg, J. Werner, S. Klausner, and A. Norman.** Oral hydralazine therapy for chronic refractory heart failure. *Circulation* 54: 879-892, 1976.
8. **Chien, S.** Role of the sympathetic nervous system in hemorrhage. *Physiol. Rev.* 47: 214-288, 1967.
9. **Guyton, A. C., C. E. Jones, and T. G. Coleman.** The pulmonary circulation in left-sided heart failure. In: *Circulatory Physiology*. Philadelphia, PA: Saunders, 1973, p. 472-475.
10. **Guyton, A. C., C. E. Jones, and T. G. Coleman.** *Circulatory Physiology: Cardiac Output and its Regulation*. Philadelphia, PA: Saunders, 1973.
11. **Guyton, A. C., A. W. Lindsey, B. Abernathy, and T. Richardson.** Venous return at various right atrial pressures and the normal venous return curve. *Am. J. Physiol.* 189: 261-269, 1957.
12. **Linderer, T., K. Chatterjee, W. W. Parmley, R. Sievers, S. A. Glantz, and J. V. Tyberg.** Influence of atrial systole on the Frank-Starling relation and the end-diastolic pressure-diameter relation of the left ventricle. *Circulation* 67: 1045-1053, 1983.
13. **Lindsey, A. W., B. F. Banahan, R. H. Cannon, and A. C. Guyton.** Pulmonary blood volume of the dog and its changes in acute heart failure. *Am. J. Physiol.* 190: 45-50, 1957.
14. **Lubbrook, P. A., J. D. Byrne, M. S. Kurnick, and R. C. McKnight.** Influence of reduction of preload and afterload by nitroglycerin on left ventricular diastolic pressure-volume relations in man. *Circulation* 56: 937-943, 1977.
15. **Maruyama, Y., K. Ashikawa, S. Isoyama, H. Kanatsuka, E. Ino-Oka, and T. Takishima.** Mechanical interactions between four heart chambers with and without the pericardium in canine hearts. *Circ. Res.* 50: 86-100, 1982.
16. **Milnor, W. R.** *Hemodynamics*. Baltimore, MD: Williams and Wilkins, 1982, p. 1-390.
17. **Nichols, W. W., and M. F. O'Rourke.** *McDonald's Blood Flow in Arteries: Theoretical, Experimental and Clinical Principles*. Philadelphia, PA: Lea and Febiger, 1990, p. 1-456.
18. **Ogilvie, R. I., and D. Zborowska-Sluis.** Effect of chronic rapid ventricular pacing on total vascular capacitance. *Circulation* 85: 1524-1530, 1992.

19. **Packer, M.** Role of the sympathetic nervous system in chronic heart failure: a historical and philosophical perspective. *Circulation* 82, Suppl. I: I1-I6, 1990.
20. **Pappenheimer, J. R., and A. Soto-Rivera.** Effective osmotic pressure of the plasma proteins and other quantities associated with the capillary circulation in the hindlimbs of cats and dogs. *Am. J. Physiol.* 152: 471-491, 1948.
21. **Piscione, F., P. G. Hugenholtz, and P. W. Surrus.** Impaired left ventricular filling dynamics during percutaneous transluminal angioplasty for coronary artery disease. *Am. J. Cardiol.* 59: 29-37, 1987.
22. **Pouleur, H., J. W. Covell, and J. Ross, Jr.** Effects of nitroprusside on venous return and central blood volume in the absence and presence of acute heart failure. *Circulation* 61: 328-337, 1980.
23. **Relman, A. S., and F. H. Epstein.** Effect of tetraethylammonium on venous and arterial pressure in congestive heart failure. *Proc. Soc. Exp. Biol. Med.* 70: 11-14, 1949.
24. **Robinson, V. J. B., O. A. Smiseth, N. W. Scott-Douglas, E. R. Smith, J. V. Tyberg, and D. E. Manyari.** Assessment of the splanchnic vascular capacity and capacitance using quantitative equilibrium blood-pool scintigraphy. *J. Nucl. Med.* 31: 154-159, 1990.
25. **Ross, J., Jr.** Acute displacement of the diastolic pressure-volume curve of the left ventricle: role of the pericardium (Editorial). *Circulation* 59: 32-37, 1979.
26. **Rutlen, D. L., E. N. Supple, and W. J. Powell, Jr.** Beta adrenergic regulation of total systemic intravascular volume in the dog. *Circ. Res.* 48: 112-120, 1981.
27. **Sagawa, K.** The ventricular pressure-volume diagram revisited. *Circ. Res.* 43: 677-687, 1978.
28. **Sagawa, K., W. L. Maughan, H. Suga, and K. Sunagawa.** *Cardiac Contraction and the Pressure-Volume Relationship.* Oxford, UK: Oxford Univ. Press, 1988, p. 1-480.
29. **Santamore, W. P., and D. Burkhoff.** Hemodynamic consequences of ventricular interaction as assessed by model analysis. *Am. J. Physiol.* 260 (*Heart. Circ. Physiol.* 29): H146-H157, 1991.
30. **Scott-Douglas, N. W., O. A. Smiseth, Y. Wang, D. E. Manyari, E. R. Smith, and J. V. Tyberg.** Venous hemodynamics of nitroglycerin in an experimental model of acute ischemic dysfunction (Abstract). *J. Am. Col. Cardiol.* 15: 87A, 1990.
31. **Shoukas, A. A.** Pressure-flow and pressure-volume relations in the entire pulmonary vascular bed of the dog determined by two-port analysis. *Circ. Res.* 37: 809-818, 1975.
32. **Shoukas, A. A. and M. C. Brunner.** Epinephrine and the carotid sinus baroreceptor reflex: influence on capacitive and resistive properties of the total systemic vascular bed of the dog. *Circ. Res.* 47: 249-257, 1980.
33. **Shoukas, A. A., and K. Sagawa.** Total systemic vascular compliance measured as incremental volume-pressure ratio. *Circ. Res.* 28: 277-289, 1971.
34. **Strobeck, J. E., and E. H. Sonnenblick.** Pathophysiology of heart failure. In: *The Ventricle: Basic and Clinical Aspects*, edited by H. J. Levine and W. H. Gaasch. Boston, MA: Nijhoff, 1985, p. 209-224.
35. **Suga, H.** Importance of atrial compliance in cardiac performance. *Circ. Res.* 35: 39-43, 1974.
36. **Sunagawa, K., W. L. Maughan, and K. Sagawa.** Effect of regional ischemia on the left ventricular end-systolic pressure-volume relationship of isolated canine hearts. *Circ. Res.* 52: 170-178, 1983.
37. **Tyberg, J. V.** Ventricular interaction and the pericardium. In: *The Ventricle: Basic and Clinical Aspects*, edited by H. J. Levine and W. H. Gaasch. Boston, MA: Nijhoff, 1985, p. 171-184.
38. **Tyberg, J. V., G. A. Misbach, S. A. Glantz, W. Y. Moores, and W. W. Parmley.** A mechanism for shifts in the diastolic, left ventricular pressure-volume curve: the role of the pericardium. *Eur. J. Cardiol.* 7, Suppl.: 163-175, 1978.
39. **Wang, Y.-D., N. W. Scott-Douglas, D. E. Manyari, E. R. Smith, and J. V. Tyberg.** Venous hemodynamics of Enalaprilat in an experimental model of acute ischemic dysfunction (Abstract). *J. Am. Col. Cardiol.* 15: 88A, 1990.
40. **Weil, M. H., and E. C. Rackow.** Pulmonary edema. In: *Cardiology*, edited by W. W. Parmley and K. Chatterjee. Philadelphia, PA: Lippincott, 1989, p. 1-12.

